JOURNAL OF CATALYSIS **65**, 318–327 (1980)

Evidence for an Oxygen Intermediate in the Catalytic Reduction of NO by CO on Rhodium Surfaces

L. H. DUBOIS, P. K. HANSMA,[1] AND G. A. SOMORJAI

Materials and Molecular Research Division, Lawrence Berkeley Laboratory, and Department of Chemistry, University of California, Berkeley, California 94720

Received November 16, 1979; revised April 14, 1980

Evidence for an oxygen intermediate in the reaction of NO and CO to form N_2 and CO_2 over rhodium surfaces is presented. High-resolution electron energy loss spectroscopy (ELS) measurements indicate that both NO and CO molecules associatively adsorb on the Rh(331) single-crystal surface at 300 K. Chemisorbed NO readily dissociates on this surface upon heating to 450 K. At 700 K high-resolution ELS and Auger electron spectroscopy both indicate that only oxygen is present on the catalyst surface. N_2 desorption below this temperature is easily detected by mass spectroscopy. The addition of CO to this surface oxygen at 700 K results in the formation of gaseous CO_2 and the removal of the surface oxygen species. Similar results were obtained when O_2 was substituted for NO as a control, indicating that oxygen is indeed a surface intermediate under our experimental conditions. The reaction mechanism to reduce NO to N_2 by CO over rhodium surfaces may then be expressed as $2NO_{(g)} \rightarrow N_{2(g)} + 2O_{(ad)}$ and $2O_{(ad)} + 2CO \rightarrow 2CO_{2(g)}$.

INTRODUCTION

The desire for clean air has stimulated both legislation and research on the reduction of nitrogen oxides (NO_x) in fossil fuel combustion exhaust. Recent interest has focused on the catalytic reduction of NO to N_2 by carbon monoxide in automobile exhaust. A promising catalyst for this reaction is rhodium (*1, 2*). The mechanism of nitric oxide reduction over Rh has been illuminated in several recent publications. Campbell and White (*3*) used thermal desorption mass spectrometry (TDS), surface titration, and steady-state reaction kinetics to study the chemisorption and reactivity of nitric oxide on a polycrystalline rhodium wire at temperatures between 330 and 950 K and at pressures below 2×10^{-8} Torr. They concluded that the mechanism must involve NO dissociation and a subsequent reaction of CO with the atomic oxygen intermediates remaining on the surface. No direct evidence for this surface oxygen species was presented, however.

Unland (*4*), Arai and Tominaga (*5*), and more recently Solymosi and Sárkány (*6*) applied infrared spectroscopy to a study of NO and CO chemisorption on alumina-supported rhodium particles. In addition to observing stretching vibrations for numerous molecular NO and CO species between 300 and 670 K and at pressures up to 150 Torr, they found an absorption band which they associated with a surface isocyanate (NCO) complex. There now is evidence for a migration of this isocyanate species from the rhodium particles to the support (*6, 7*). Finally, Iizuka and Lunsford (*8*) studied the reduction of nitric oxide by carbon monoxide to form N_2O and CO_2 over rhodium–Y zeolites. They proposed a $[Rh^I(CO)_2NO]^+$ complex as a reaction intermediate based on infrared spectroscopic evidence. The spectral range of all of these studies did not extend to the region below 1000 cm^{-1} where vibrations from surface N and O atoms from dissociated nitric oxide would be expected. Thus these studies neither supported nor contradicted the pre-

---

[1] On sabbatical leave from the Department of Physics, University of California, Santa Barbara, Calif. 93106.

0021-9517/80/100318-10$02.00/0

vious evidence for the presence of a surface oxygen intermediate.

An adsorbed oxygen species from NO dissociation has been observed on the surface of other transition metals. Thomas and Weinberg (*9*) reported such a species on the Ru(001) single-crystal surface using high-resolution electron energy loss spectroscopy (ELS). Zhdan *et al.* (*10, 11*) observed a similar species on the Ir(111) surface with both X-ray and ultraviolet photoelectron spectroscopy. These authors argue convincingly for a surface oxygen intermediate in the reduction of NO by CO over iridium catalysts.

In this paper we report on studies of the molecular chemisorption and subsequent dissociation of nitric oxide on a Rh(331) single-crystal surface. Here we combine high-resolution ELS and Auger electron spectroscopy (AES) to determine the structure and chemical composition of the adsorbed species with TDS and kinetic studies to monitor the reaction products after desorption into the gas phase. These new high-resolution ELS and AES measurements on a single-crystal rhodium surface complement the previous studies (*1–6, 8*) to present a complete picture of a mechanism involving a surface oxygen intermediate under our reaction conditions.

EXPERIMENTAL

Experiments were carried out in an ion-pumped stainless-steel ultrahigh-vacuum chamber built in two levels. The upper portion contained the standard single-crystal surface analysis equipment (four grid LEED/Auger optics, glancing-incidence electron gun, and quadrupole mass spectrometer). After dosing, the sample was lowered into the high-resolution electron energy loss spectrometer by an extended-travel precision manipulator. The ELS spectrometer consists of two 127° cylindrical sectors modified to meet second-order image aberration and fringe field corrections (*12*). Details of the spectrometer design are presented elsewhere (*13*). In the present series of experiments the electron beam has an energy of approximately 5 eV and the angle of incidence is fixed at 65° to the surface normal. Electrons are only collected in the specular direction. The elastic scattering peak has a full width at half maximum between 60 and 100 cm^{-1} and a maximum intensity of 1×10^5 counts/sec.

The procedures for sample preparation, mounting, and cleaning have been described previously (*14*). Briefly, the Rh(331) crystal, oriented to $\pm\frac{1}{2}°$, was cleaned by a combination of argon ion bombardment (1000–2000 eV) followed by annealling in vacuum and O_2 (800–1000 K) to remove carbon, sulfur, and boron. Using the stepped-surface notation of Lang *et al.* (*15*) this crystal plane can be viewed as a Rh(S)–[3(111) × (111)] surface. The three-atom-wide (111) terraces are uniformly spaced by monoatomic-height steps also of (111) orientation. A real-space drawing of this surface is presented in Ref. (*14*).

NO, CO, and O_2 adsorptions were studied at pressures between 1×10^{-8} and 1×10^{-7} Torr and at temperatures between 300 and 900 K. Neither gas exposures nor background pressures were corrected for ion gauge sensitivity.

TDS spectra were recorded at an initial heating rate of 40 K/sec. Kinetic studies were performed by predosing the Rh(331) surface with either O_2 or NO at 700 K and initiating the CO flow at $t = 0$. The CO_2 partial pressure ($m/e = 44$) was monitored with a mass spectrometer located approximately 15 cm from the crystal.

RESULTS AND DISCUSSION

A. *The Molecular Chemisorption of NO on Rhodium*

The lowest trace of Fig. 1 shows the high-resolution ELS spectrum from the adsorption of 1 L (1 L = 1 Langmuir = 10^{-6} Torr · sec = 1.33×10^{-4} Pa · sec) of NO on the initially clean Rh(331) single-crystal surface at 300 K. The strong band above 1700 cm^{-1}

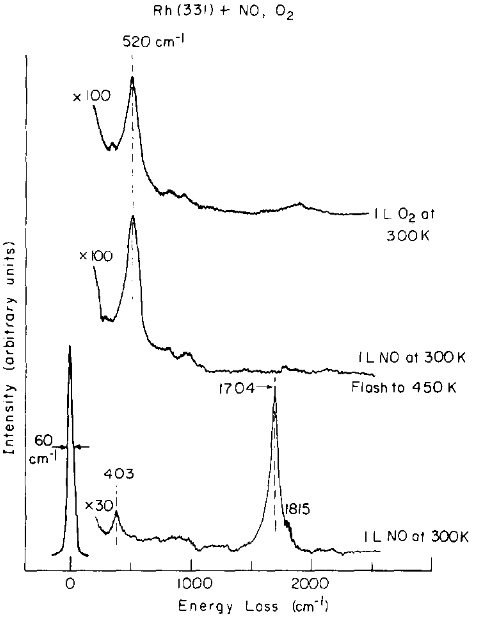

FIG. 1. Nitric oxide molecularly adsorbs on the Rh(331) single-crystal surface at 300 K as shown by the presence of N-O stretching vibrations (1704, 1815 cm^{-1}) in the bottom high-resolution ELS spectrum. This species dissociates by 450 K as indicated by the absence of the N-O stretching vibrations in the middle spectrum. The 520-cm^{-1} peak in this spectrum is similar to that obtained from the adsorption of O_2 gas at 300 K (top spectrum).

is typical of a N-O stretching vibration for molecularly adsorbed nitric oxide (*16*). By comparison with the infrared spectra of model nitrosyl compounds of known molecular structure, we can assign the 1704-cm^{-1} loss to a terminally bonded NO species (*20, 21*). The Rh—N═O bond is most likely bent (*18, 20, 21*), but the exact angle cannot be determined here. Using a similar analysis, the small shoulder at 1815 cm^{-1} can be assigned to a linear nitrosyl species. The weak band at 403 cm^{-1} is characteristic of a metal–nitrogen bending mode for an associatively adsorbed species (*17, 18*). This is in agreement with the observation of a bent nitrosyl. The normal dipole selection rule (*22*) would not allow the observation of such a mode if the adsorbate was bonded perpendicular to the surface. The metal–nitrogen stretching vibration from such a species is expected to be 100–200 cm^{-1} lower in frequency (*18*). The results of detailed infrared studies on numerous nitrosyl compounds have been reviewed recently by Pirug *et al.* (*18*). They conclude that the experimental data on both the halogen nitrosyls and the transition metal nitrosyls provide evidence for well-separated M—N═O bending and stretching frequencies with the latter always lower than the former.

Based on the coordination chemistry of metal nitrosyls, one can postulate a large number of nitric oxide-bonding geometries on rhodium surfaces. These include linear-, bent-, and bridge-bonded NO, as well as formation of NO^+ and NO^- species (*20, 23*). Infrared studies have identified a variety of these species on alumina-supported rhodium catalysts (*4–6*). Characteristic N—O stretching frequencies have been tabulated by Arai and Tominaga (*5*). We have now observed the formation of at least five different NO species on the Rh(111) surface using high-resolution ELS (*19*). Each species is stable on the surface over a small temperature and coverage range. Because of the "relative simplicity" of the NO vibrational spectrum on the (331) plane of rhodium we have decided to pursue our catalytic studies on this surface. The reasons for the differences in the nature of NO bonding to the various crystal faces of rhodium are a promising area for future research.

The conclusions of this paper do not, however, hinge on a detailed assignment of the observed energy loss peaks. The point we wish to make here is that nitric oxide molecularly chemisorbs on the Rh(331) surface at 300 K.

Both the relative intensities and the positions of the energy loss peaks in the lower trace of Fig. 1 were found to be essentially independent of gas exposure (from 0.1 to 10 L). The integrated intensity of the ELS peak does increase with increasing gas dosage, however. Absolute nitric oxide coverages were not determined.

B. The Dissociation of NO on Rhodium

As the rhodium substrate is heated above 450 K the molecular NO vibrational bands in the lower trace of Fig. 1 disappear and a single peak near 520 cm^{-1} appears (Fig. 1, middle trace). The disappearance of the high-frequency mode and the simultaneous appearance of the 520-cm^{-1} band clearly indicate the dissociation of nitric oxide. Furthermore, at least one of the dissociation products must remain on the surface. The upper trace in Fig. 1 shows the vibrational spectrum from the adsorption of 1 L of O_2 on the Rh(331) surface at room temperature. A single band at 520 cm^{-1} due to dissociatively chemisorbed oxygen (*14*) is visible. This suggests that the 520-cm^{-1} band produced from NO dissociation is due to surface oxygen. The absence of a second peak is not necessarily evidence for nitrogen desorption since it is thought that the M–N stretch from dissociated NO should be weak (*9*). This peak could be hidden beneath the relatively intense rhodium–oxygen stretch.

We could not detect either the molecular or the dissociative chemisorption of dinitrogen on the Rh(331) single-crystal surface at 300 K at N_2 exposures up to 10^4 L. Mimeault and Hansen (*24*) found that dinitrogen could adsorb on a polycrystalline rhodium wire upon activation with a hot tungsten filament. This has also been reported recently by Campbell and White (*3*). Due to the long distance (~15 cm) and the relatively low temperature of our thoriated-iridium mass spectrometer and ion gauge filaments, we were unable to detect any activated nitrogen adsorption, even at N_2 exposures greater than 10^4 L. Thus we could not measure the atomic nitrogen vibrational spectrum. However, the absence of surface nitrogen in the middle vibrational spectrum of Fig. 1 can be confirmed by thermal desorption mass spectrometry and by Auger electron spectroscopy.

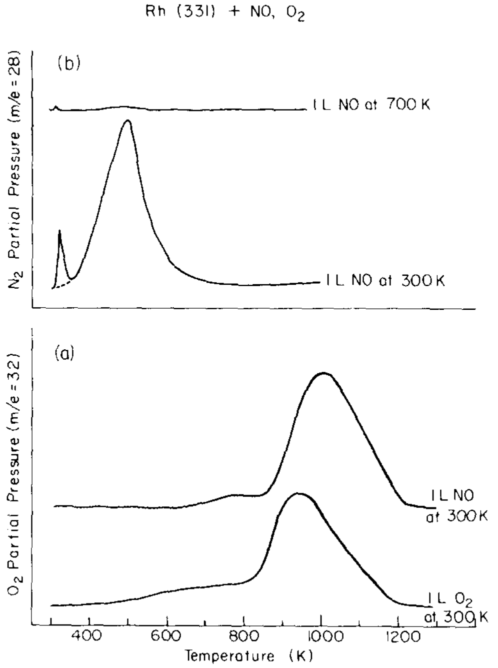

FIG. 2. (a) O_2 desorption (m/e = 32) from the adsorption of 1 L of either O_2 (lower trace) or NO (upper trace) on the Rh(331) single-crystal surface at 300 K. (b) N_2 desorption (m/e = 28) from the adsorption of 1 L of NO at either 300 K (lower trace) or 700 K (upper trace). The small peak at 325 K is presumably due to nitrogen desorption from the crystal support wires.

Figure 2 displays TDS spectra for N_2 and O_2 desorption from the Rh(331) single crystal after exposing the surface to 1 L of NO. Note that if NO is adsorbed at room temperature the nitrogen desorbs as N_2 (m/e = 28) below 500 K (Fig. 2b) while the oxygen desorbs as O_2 (m/e = 32) (Fig. 2a) only at much higher temperatures. Figure 2a also shows that O_2 desorption is similar whether the rhodium surface is exposed to gaseous nitric oxide or to oxygen. The NO (m/e = 30) TDS spectrum showed only one peak near 460 K. N_2O (m/e = 44) desorption from this surface has also been reported (*14*). Similar thermal desorption results have been obtained previously both by Campbell and White (*3*) on polycrystalline rhodium wire and by Castner and Somorjai (*14*) on stepped rhodium single-crystal surfaces during NO chemisorption studies. Finally, note that if NO is adsorbed on the rhodium surface at 700 K (a typical reaction temperature for an automobile catalytic converter) and the crystal cooled to 300 K, subsequent flashing yields negligible nitrogen desorption from the surface (Fig. 2b). This is consistent with the relatively low temperature found for N_2 desorption from adsorbed NO.

The absence of surface nitrogen is also confirmed by Auger electron spectroscopy (see Fig. 3). The chemisorption of 1 L of NO on the Rh(331) single-crystal surface at 300 K (lower trace) results in both nitrogen and oxygen present on the surface (*25*). This is consistent with the molecular chemisorption of nitric oxide indicated by the vibrational spectra in Fig. 1. Chemisorption of 1 Langmuir of NO at 700 K results in only oxygen present on the surface (upper trace). Both the TDS and the AES results lead us to conclude that the peak at 520 cm^{-1} in the middle trace of Fig. 1 is due solely to adsorbed oxygen.

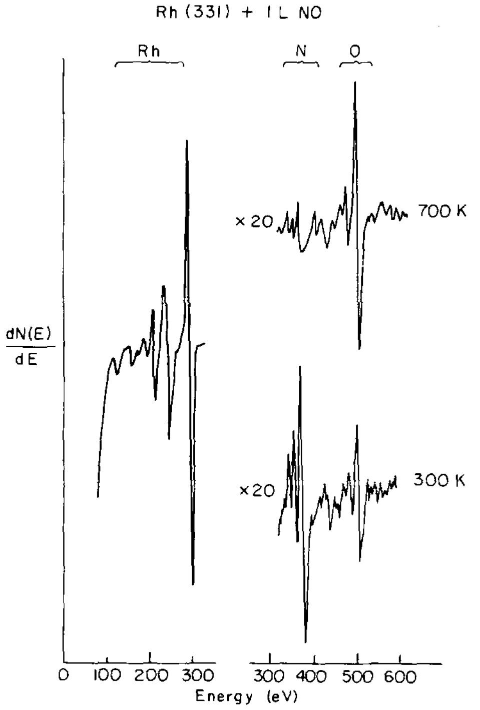

FIG. 3. The Auger spectrum of NO chemisorbed on the initially clean Rh(331) single-crystal surface shows both nitrogen and oxygen peaks when adsorbed at 300 K, but only oxygen transitions when adsorbed at 700 K. The fine structure between the primary peaks is irreproducible and presumably due to noise.

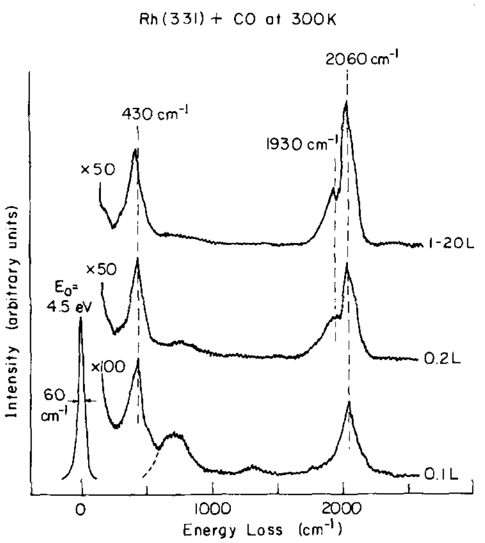

FIG. 4. Carbon monoxide molecularly adsorbs on the Rh(331) single-crystal surface at 300 K. At a 0.1-L exposure (lower trace) CO is linearly bonded to single rhodium atoms on the (111) terraces ($\nu_{C=O}$ = 2060 cm^{-1}). The 430-cm^{-1} loss is the Rh–CO stretching and/or bending vibration for this species. The broad band centered near 800 cm^{-1} (dashed line) may be caused by electron reflection from the outer half of the analyzer (see text) (*12*). Above a 0.2-L CO exposure (middle trace) carbon monoxide molecules bonded to rhodium step atoms are formed ($\nu_{C\equiv O}$ = 1930 cm^{-1}). The room-temperature spectra do not change up to a 20-L CO exposure (upper trace).

Thus at a typical operating temperature for a catalytic converter (700 K) the adsorption of NO results in the liberation of N_2 gas and in the formation of a stable surface oxygen species. Vibrational spectra recorded after flashing the crystal to successively higher temperatures indicate that the metal–oxygen stretch is visible until above 850 K.

C. The Chemisorption of CO on Rhodium

Much effort has gone into understanding the vibrational spectrum of carbon monoxide chemisorbed on rhodium. A review of previous work is presented elsewhere (*26, 27*) and will not be repeated here. The lowest trace of Fig. 4 shows the high-resolution ELS spectrum from the adsorption of 0.1 L of CO on the initially clean Rh(331) single-crystal surface at 300 K. Only two losses at 430 and 2060 cm^{-1} are visible. The broad peak (dashed line) centered near 800 cm^{-1} is most likely due to electron reflection from the outer half of the analyzer (*12*). The causes of this peak are discussed in detail by Froitzheim *et al.*(*12*). By comparison with the infrared spectra of model organometallic compounds of known molecular structure (*26, 27*) we can assign the 2060-cm^{-1} loss to the carbon–oxygen stretching vibration of a linearly bonded CO species. The 430-cm^{-1} loss is the rhodium–carbon stretching and/or bending vibration for this species (*28, 29*). ELS spectra of CO chemisorbed on the (111) plane of rhodium also show the presence of linearly bonded carbonyl species (*26*). Molecular CO desorbs from both of these surfaces with first-order kinetics and with an activation energy of 31 kcal/mole (*14, 26, 30*). This activation energy decreases with increasing coverage on both surfaces as well (*13, 26, 30*). Therefore, we conclude that at low CO exposures carbon monoxide is molecularly adsorbed on the Rh(331) single-crystal surface and is linearly bonded to a single rhodium atom on the (111) terraces.

The middle trace of Fig. 4 shows that by a 0.2-L CO exposure a third energy loss peak at 1930 cm^{-1} is observed. A detailed assignment of this mode is difficult at present. Linearly bonded rhodium carbonyls (Rh—CO) have C≡O stretching frequencies near 2060 cm^{-1} while bridge-bonded species ($Rh_2{>}CO$) have C═O stretching frequencies at 1870 cm^{-1} (*26, 27*). However, both Pearce (*27*) and Yang and Garland (*31*) observed a similar mode (1925 cm^{-1}) in the infrared spectra of CO chemisorbed on either silica- or alumina-supported rhodium particles. These authors found that the intensity of the mode decreased as the sample reduction temperature increased and the particle sizes became larger (*27, 31*). Both groups assigned this peak to a bridge-bonded species. Pearce (*27*) suggested that sintering removes the high-index planes on which this bridged species adsorbs. In agreement with this, we have only observed the 1930-cm^{-1} mode on the stepped Rh(331) surface and not on the flat Rh(111) surface. This species may be located along the step edges or at least be associated with the step atoms. The results of recent low-energy electron diffraction (LEED), thermal desorption mass spectrometry, and Auger electron spectroscopy studies also lead us to this conclusion (*14*).

Castner and Somorjai (*14*) showed that the chemisorption of carbon monoxide on the Rh(331) surface formed a series of well-ordered LEED patterns at 300 K. A hexagonal overlayer of carbon monoxide molecules is seen at all coverages. A proposed mechanism for the transformation between ordered structures is by compression of the hexagonal layer parallel to the step edge (*14*). This would require that the ratio of occupied terrace sites to occupied step sites remains approximately constant over the entire coverage range. This is precisely what we see in the vibrational spectra: the intensity ratio of the 2060-cm^{-1} loss to the 1930-cm^{-1} loss does not significantly change with increasing CO exposure (up to at least 20 L of CO (Fig. 4, top)). Furthermore, this intensity ratio (~2.5 : 1) is in reasonable agreement with the ratio of the number of exposed rhodium terrace atoms to step atoms (~2.3 : 1).

Recent TDS and AES studies indicate that carbon monoxide can dissociate on both stepped single-crystal ((331), (755)) (*14*) and polycrystalline (*32*) rhodium samples, but not on the Rh(111) surface (*26, 30, 33*) at elevated temperatures under ultrahigh-vacuum conditions. Recall that we only see the 1930-cm^{-1} mode on the stepped Rh(331) surface and not on the flat Rh(111) surface. This peak completely disappears upon flashing a CO-saturated surface to 450 K in vacuum. This is well below the temperature for carbon monoxide desorption from the low-index terraces of the crystal (*14, 26, 30*). (The TDS peak maximum occurs at ~550 K, depending on initial surface coverage and heating rate.) Erley *et al.* (*34*) have shown that low-frequency C≡O stretching vibrations on nickel surfaces can be associated with the chemisorption of carbon monoxide at step sites. These species also can be dissociated by heating the sample to 430 K in vacuum. All of these studies are consistent with the assignment of the 1930-cm^{-1} mode to the C≡O stretching vibration of a carbon monoxide molecule chemisorbed along or near the step edge.

Again, the conclusions of this paper do not hinge on a detailed assignment of the observed energy loss peaks since high-resolution ELS and TDS studies indicate that neither the linear nor the "step" CO species is present on the surface at 700 K under ultrahigh-vacuum conditions. The important point here is that carbon monoxide molecularly chemisorbs on the Rh(331) single-crystal surface at 300 K. Step sites may play an important role in the catalytic chemistry of rhodium surfaces at elevated temperatures however.

D. *The Interaction of CO with Molecular NO*

The coadsorption of NO and CO on the Rh(331) surface at 300 K yields vibrational spectra that are essentially the sum of Figs. 1 and 4. The frequencies of the N═O and C≡O stretching vibrations are shifted downward slightly when compared to the values measured in Figs. 1 and 4. Small peak shifts have also been seen in the ELS spectra of NO and CO coadsorbed on the (001) face of ruthenium (*35*). No energy loss peaks corresponding to new surface species are observed. Specifically, the characteristic stretching vibrations of surface NCO and Rh(CO)(NO) are not seen (*4*–*6*). Such species are reported to form on supported rhodium catalysts, but only at elevated temperatures and pressures (*4*–*6*). High-resolution ELS studies indicate that the sequential adsorption of NO and CO (either NO followed by CO or the reverse) at 300 K did not yield any new surface species either. It is interesting to note that the NO-saturated Rh(331) surface inhibited all CO adsorption while the bent nitrosyl species could still find a few open sites on the CO-saturated surface. This bent NO species could also form on an oxygen-pretreated rhodium surface. Reference (*3*) contains an extensive discussion of TDS and low-pressure kinetic studies on the NO + CO system.

E. *The Reaction of CO with Dissociated NO*

Carbon monoxide readily reacts with the oxygen remaining on the surface after NO dissociation. Figure 5 shows what happens to the Rh–O stretching vibration as CO is added to either dissociatively chemisorbed O_2 (a) or NO (b) at 700 K. Note that in both cases the intensity of the 520-cm^{-1} loss is measurably decreased by a 1-L CO exposure and has disappeared into the noise by a 5-L CO exposure. Surface oxygen produced during O_2 chemisorption is more easily removed than surface oxygen formed as a result of the dissociation of NO. This is a reproducible effect that will be discussed in more detail below.

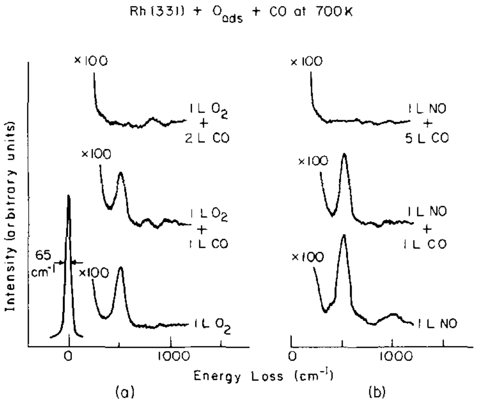

FIG. 5. The 520-cm^{-1} peak in the high-resolution ELS spectra of either O_2 (a) or NO (b) adsorbed on the Rh(331) single-crystal surface at 700 K decreases rapidly upon exposure to gas-phase carbon monoxide.

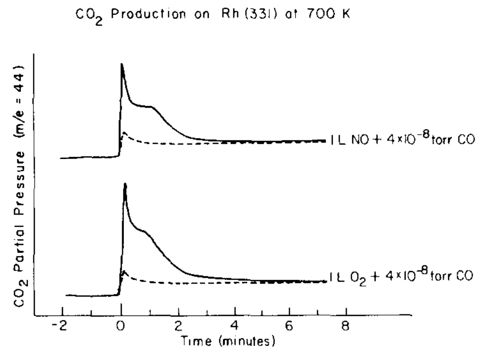

FIG. 6. Gaseous CO_2 production on the Rh(331) surface at 700 K after predosing the crystal with 1 L of either O_2 (lower trace) or NO (upper trace). 4×10^{-8} Torr of CO is admitted to the vacuum chamber at $t = 0$ and CO_2 production is monitored by mass spectroscopy ($m/e = 44$). The dashed curves show the background CO_2 liberation if the surface was not preexposed to either NO or O_2 before CO admission.

We carried out a kinetic study to determine which gases are produced when CO reacts with surface oxygen. In Fig. 6 the rhodium substrate was first heated to 700 K and then dosed with either 1 L of O_2 (lower trace) or NO (upper trace) to produce a surface oxygen species. The reaction products were monitored with a mass spectrometer as 4×10^{-8} Torr of CO was admitted to the vacuum chamber at $t = 0$. As one might expect, carbon dioxide ($m/e = 44$) was the primary product. CO_2 was produced until the CO exposure was of the order of 5 L (2 min at 4×10^{-8} Torr). This observation correlates with the high-resolution electron energy loss results of Fig. 5 which showed that the surface oxygen disappeared by a 5 L CO exposure.

There is evidence that CO reacts with adsorbed oxygen directly from the gas phase (an Eley–Rideal mechanism) as well as after being adsorbed on the surface (a Langmuir–Hinshelwood mechanism). Campbell *et al.* (*36, 37*) studied the reaction between adsorbed oxygen and carbon monoxide over polycrystalline rhodium wires. They concluded that the formation of carbon dioxide proceeded by both Langmuir–Hinshelwood and Eley–Rideal kinetics, depending on substrate temperature and gas pressure. They also found both mechanisms to be operative in their recent investigation of the catalytic reduction of NO by CO over polycrystalline rhodium wires (*3*).

The dashed lines in Fig. 6 represent the background reactivity of both the rhodium single-crystal surface and the mass spectrometer filaments without predosing the sample with either O_2 or NO. The initial spike in all of these traces is caused by reactions taking place either on the edges of the rhodium crystal or on the sample support wires. Due to our resistive heating methods both of these areas are warmer than the front surface of the crystal.

F. The Reaction Mechanism

From the above we conclude that under our experimental conditions the reaction of NO and CO to form N_2 and CO_2 proceeds by the following two consecutive steps:

$$2NO_{(g)} \rightarrow N_{2(g)} + 2O_{(ad)}, \qquad (1)$$

$$2O_{(ad)} + 2CO \rightarrow 2CO_{2(g)}. \qquad (2)$$

In the present study we have sequentially reacted nitric oxide and carbon monoxide over the Rh(331) surface to form gaseous dinitrogen and carbon dioxide. This reaction can be run continuously by heating our rhodium crystal to 700 K in 5×10^{-7} Torr of a 1 : 1 NO : CO mixture. Unfortunately, due to the rapid reaction of these gases on the mass spectrometer filaments, we could not perform meaningful kinetic studies with the present apparatus.

An interesting feature of the data is that surface oxygen from NO desorbs at a slightly higher temperature (Fig. 2a, Refs. (*3, 14*)) than the surface oxygen from dissociated NO. The 60 K shift in the O_2 peak temperature cannot be accounted for by different surface oxygen concentrations since the integrated areas of the two desorption peaks in Fig. 2a agree to within 5%. Surface oxygen from NO also reacts somewhat less readily with CO (Figs. 5 and

6) than the surface oxygen from dissociated O_2. Though we do not understand these effects, they are consistent with recent kinetic studies on supported rhodium catalysts under simulated reaction conditions (*1*). Specifically, the rate of conversion of NO to N_2 and CO_2 by the reaction with CO is less than the rate of conversion of O_2 to CO_2 by CO under identical experimental conditions (*1*). In contrast, on iridium, the rate of reaction of NO with CO is higher than that of O_2 (*1*). Further research into the mechanism of this reaction selectivity might be both scientifically interesting and technologically important.

SUMMARY

The following evidence for a surface oxygen intermediate in the reaction $2NO_{(g)} + 2CO_{(g)} \rightarrow N_{2(g)} + CO_{2(g)}$ was presented:

(a) NO dissociates on the Rh(331) single-crystal surface below 450 K, well below typical catalytic converter reaction temperatures of 600–800 K (Fig. 1).

(b) The nitrogen from dissociated NO desorbs as N_2 below 500 K (Fig. 2).

(c) The oxygen from dissociated NO is stable on the surface at typical reaction temperatures in vacuum (Figs. 2, 3, and 5).

(d) The oxygen from dissociated NO is readily removed by CO under our experimental conditions (Fig. 5).

(e) The reaction of CO with the surface oxygen produces gaseous CO_2 (Fig. 6).

The reaction mechanism may now be expressed as $2NO_{(g)} \rightarrow N_{2(g)} + 2O_{(ad)}$ and $2O_{(ad)} + 2CO \rightarrow 2CO_{2(g)}$. Key to this mechanism is the identification of the 520-cm^{-1} peak as surface oxygen in the high-resolution electron energy loss spectrum resulting from the dissociation of adsorbed NO (Fig. 1, middle trace; Figs. 5 and 6). This identification is supported by:

(a) the presence of a similar 520-cm^{-1} peak from the adsorption of O_2 (Fig. 1);

(b) thermal desorption traces indicating that nitrogen from dissociated NO desorbs at a temperature below temperatures at which this peak is stable (Fig. 2);

(c) AES results showing only oxygen and the clean rhodium surface features when the 520-cm^{-1} peak is present (Fig. 3); and

(d) kinetic studies indicating that the 520-cm^{-1} peak from dissociated NO was removed with similar (but not identical) kinetics to that from adsorbed O_2 (Figs. 5 and 6).

Although there can be little doubt that this reaction mechanism operates in high vacuum, it is not clear that it is the predominant mechanism on rhodium catalysts under automobile exhaust operating conditions. Furthermore, we cannot rule out a number of the possible mechanisms proposed by other authors. However, recent studies on Pt/SiO_2 catalysts under high-pressure reducing conditions found kinetics and product selectivities in good agreement with a mechanism based upon the dissociation of NO as the rate-limiting step (*7*).

ACKNOWLEDGMENTS

We thank Professor A.T. Bell, Professor W. H. Weinberg, and Dr. R. M. Kroeker for helpful discussions. P.K.H. acknowledges the Alfred P. Sloan Foundation, the Division of Materials Research of the National Science Foundation, and the Office of Naval Research for support. This work was supported by the Division of Materials Sciences, Office of Basic Energy Sciences, United States Department of Energy.

REFERENCES

1. Taylor, K. C., and Schlatter, J. C., *J. Catal.*, **63,** 53 (1980).

2. Hegedus, L. L., Summers, J. C., Schlatter, J. C., and Baron, K., *J. Catal.* **56,** 321 (1979).

3. Campbell, C. T., and White, J. M., *Appl. Surface Sci.* **1,** 347 (1978).

4. Unland, M. L., *J. Catal.* **31,** 459 (1973); *J. Phys. Chem.* **79,** 610 (1975).

5. Arai, H., and Tominaga, H., *J. Catal.* **43,** 131 (1976).

6. Solymosi, F., and Sárkány, J., *Appl. Surface Sci.* **3,** 68 (1979).

7. Lorimer, D., and Bell, A. T., *J. Catal.* **59,** 233 (1979).

8. Iizuka, T., and Lunsford, J. H., *J. Mol. Catal.*, in press.

9. Thomas, G. E., and Weinberg, W. H., *Phys. Rev. Lett.* **41,** 118 (1978).

10. Zhdan, P. A., Boreskov, G. K., Egelhoff, W. F., Jr., and Weinberg, W. H., *J. Catal.* **45,** 281 (1976).

11. Zhdan, P. A., Boreskov, G. K., Boronin, A. I., Schepelin, A. P., Egelhoff, W. F., Jr. and Weinberg, W. H., *Appl. Surface Sci.* **1,** 25 (1977).

12. Froitzheim, H., Ibach, H., and Lehwald, S., *Rev. Sci. Instrum.* **46,** 1325 (1975).

13. Dubois, L. H., and Somorjai, G. A., ACS Symposium Series, (A. T. Bell and M. L. Hair, Eds.). Amer. Chem. Soc. Washington, D. C., 1980, in press.

14. Castner, D. G., and Somorjai, G. A., *Surface Sci.* **83,** 60 (1979).

15. Lang, B., Joyner, R. W., and Somorjai, G. A., *Surface Sci.* **30,** 454 (1972).

16. Vibrational spectra of associatively adsorbed NO have been recorded on the Pt(111) (*17*), Pt(100) (*18*), Ni(111) (*19*), Ru(001) (*9*), and Rh(111) (*19*) single-crystal surfaces.

17. Ibach, H., and Lehwald, S., *Surface Sci.* **76,** 1 (1976).

18. Pirug, G., Bonzel, H. P., Hopster, H., and Ibach, H., *J. Chem. Phys.* **71,** 593 (1979).

19. Dubois, L. H., and Hansma, P. K., unpublished observations.

20. Cotton, F. A., and Wilkinson, G., "Advanced Inorganic Chemistry," 3rd ed. Wiley, New York, 1972.

21. Nakamoto, K., "Infrared and Raman Spectra of Inorganic and Coordination Compounds," 3rd ed. Wiley, New York, 1978.

22. Pearce, H. A., and Sheppard, N., *Surface Sci.* **59,** 205 (1976).

23. Eisenberg, R., and Meyer, C. D., *Accounts Chem. Res.* **8,** 26 (1975).

24. Mimeault, V. J., and Hansen, R. S., *J. Phys. Chem.* **70,** 3001 (1966).

25. "Handbook of Auger Electron Spectroscopy," 2nd ed. Physical Electronics Industries, Eden Prairie, Minn., 1978.

26. Dubois, L. H., and Somorjai, G. A., *Surface Sci.* **91,** 514 (1980).

27. Sheppard, N., and Nguyen, T. T., *in* "Advances in Infrared and Raman Spectroscopy" Vol. 5 (R. J. H. Clark and R. E. Hester, Eds.), p. 67. Heyden & Son, London, 1978.

28. Kroeker, R. M., Kaska, W. C., and Hansma, P. K., *J. Catal.* **57,** 72 (1979); *J. Catal.* **61,** 87 (1980).

29. Dubois, L. H., Hansma, P. K., and Somorjai, G. A., *Appl. Surface Sci.*, in press.

30. Thiel, P. A., Williams, E. D., Yates, J. T., Jr., and Weinberg, W. H., *Surface Sci.* **84,** 54 (1979).

31. Yang, A. C., and Garland, C. W., *J. Chem. Phys.* **61,** 1504 (1957).

32. Sexton, B. A., and Somorjai, G. A., *J. Catal.* **46,** 167 (1977).

33. Yates, J. T., Jr., Williams, E. D., and Weinberg, W. H., *Surface Sci.* **91,** 562 (1980).

34. Erley, W., Ibach, H., Lehwald, S., and Wagner, H., *Surface Sci.* **83,** 585 (1979).

35. Thiel, P. A., Weinberg, W. H., and Yates, J. T., Jr., *J. Chem. Phys.* **71,** 1643 (1979).

36. Campbell, C. T., and White, J. M., *J. Catal.* **54,** 289 (1978).

37. Campbell, C. T., Shi, S.-K., and White, J. M., *Appl. Surface Sci.* **2,** 382 (1979).